Growth of eigenmodes with moderate mode numbers in nonlinear MHD simulation of LHD

Hideaki MIURA[1)] and Noriyoshi NAKAJIMA[1)]

[1)]*National Institute for Fusion Science, Toki 509-5292, Japan*

(Received 15 October 2007)

Direct numerical simulations of compressible, nonlinear magnetohydrodynamic equations in the fully three-dimensional geometry of the large helical device are carried out to study the linear and nonlinear growth of the pressure-driven instability. Two parameter sets are adopted in the simulation study. One parameter set provides small dissipative coefficients so that the simulation results can be compared to the ideal linear stability analysis. By the use of this parameter set, the growth rates in the linear stage of our simulation coincides with the ideal linear growth rates. Another parameter set is provided to study nonlinear evolutions. Excitations of flows parallel to the magnetic field, its role to the nonlinear saturations are studied.

Keywords: direct numerical simulation, MHD instability

DOI: 10.1585/pfr.1.001

1 Introduction

In researches of magnetic confinement devices such as the Large Helical Device (LHD), Magnetohydrodynamics (MHD) instability is one of the key issues to understand plasma behaviors in the devices. Aiming to clarify the physics of the MHD activities observed in the LHD experiments[1], many linear analysis and nonlinear simulations have been carried out [2, 3, 4, 5, 6]. Because of the short wave instability nature of the the pressure driven instability, small scales must be sufficiently resolved in a numerical computation. In the numerical study of an instability, the linear growth rate is an important index. In linear analysis of an ideal MHD system, high mode behaviors can be well predicted. However, in numerical simulations, non-ideal (dissipative) MHD equations are studied because the dissipation is indispensable to avoid numerical instability. Since the resolution available in a numerical simulation are restricted, the dissipative coefficients in simulations are often far larger than the values expected to compare numerical results to experimental results. Typically, the adoption of the large coefficients brings about unfavorable damping of high modes.

In our recent work on nonlinear MHD simulations of LHD by the use of the MHD In Non-Orthogonal System (MINOS) code[3], the growth rate of the lowest mode coincides well with the linear ones obtained by the CAS3D code.[4] However, the growth rates of moderate and high modes in the simulation are apparently suppressed by the viscosity and the coincidence is lost as the mode number becomes larger. In this paper, the number of the grid points of our simulations is increased to study the moderate modes behaviors. Numerical simulations are carried out for the equilibrium magnetic field with the vacuum magnetic axis position $3.6m$ and the pressure profile $p(\psi) = (1 - \psi^2)$ where the ψ is the toroidal magnetic flux. Growth of the moderate mode numbers, generation of toroidal flows and nonlinear saturations of the instability are discussed. In this articles, two parameter sets are adopted: (A) the isotropic heat conductivity $\kappa = 1 \times 10^{-6}$ (that is, the parallel heat conductivity $\kappa_{//}$ and the perpendicular heat conductivity $\kappa_{\perp}$ is identical), the resistivity $\eta = 1 \times 10^{-6}$, the viscosity $\mu = 1 \times 10^{-6}$, and (B) $\kappa_{//} = 1 \times 10^{-2}$, $\kappa_{\perp} = 1 \times 10^{-6}$, $\eta = 1 \times 10^{-6}$, $\mu = 1 \times 10^{-4}$. These parameters are already normalized by some typical quantities (see Ref.[5]) and hence the reciprocal of the dissipative number can be considered as some similarity parameters such as the Reynolds number $Re = 1/\mu$ and the Lundquist number $S = 1/\eta$. The number of grid points are 193×193 on a poloidal cross-section and 640 in the toroidal direction. The number of grid points is doubled in the two directions of a poloidal cross-section compared to our earlier works.[5, 6] The parameter set (A) provides a high Reynolds number and the behaviors of the solutions may be easily compared to an ideal linear analysis. Though the simulation with this parameter set cannot be completed because the numerical resolution (number of grid points) is not sufficient for such a high Reynolds number flow, it serves to study linear stages. The parameter set (B) provides the moderate Reynolds number and nonlinear saturation within the numerical resolution, although the linear stage is influenced by the dissipative coefficients μ and $\kappa_{//}$. Thus we first study the former case, parameter set (A) so that the linear growth are clearly seen. Then the nonlinear growth is studied for the parameter set (B).

author's e-mail: miura.hideaki@nifs.ac.jp

2 Comparison to linear ideal analysis

Here we study the growth of Fourier amplitudes of the velocity vector. The velocity vector field $\boldsymbol{V}$ is decomposed into the normal ($V_{\nabla\psi}$), the parallel (V_b) and the binormal components ($V_{\nabla\psi\times b}$) Then each of the three vector components are decomposed into the Fourier modes m and n on the Boozer coordinate. By the use of the Fourier coefficient $V_{\alpha,mn}(\psi)$, the power spectrum $A_{\alpha,n} = \sum_m \int^{\psi} V^2_{i,mn} d\psi$ is defined.[5] In Fig.1(a), the time evolution of the volume-integrated amplitudes of the three vector components of the velocity vector field are shown for the parameter set (A). Hereafter, the abscissa t is normalized by the toroidal Alfven time τ_A whenever a time series is plotted. In Fig.1(b), the time evolutions of $A_{\alpha,n}$ are shown. Here we recall that a single Fourier mode on the Boozer coordinate is not the linear eigen-function of the MHD equations by itself. A linear eigen-function consists of multiple Fourier modes, as are shown by Nakajima[8]. However, as is shown in the reference, the toroidal coupling in the LHD is so weak that the poloidal Fourier wavenumber n can be approximately recognized as a good quantum number. Based on this understanding, we see only the n-wavenumber dependence of the Fourier amplitude growth by summing m over all wavenumbers. Fig.1(c) is the magnification of the linear stage of this simulation. Observe in Figs.1(b) and (c) that some of the Fourier amplitudes achieve exponential growth while some show further acceleration. Because of the high Reynolds number $1/\mu = 10^6$, the computation is terminated in the midst of the growth. However, observations of the growth of the energy faster than an exponential growth in Figs.1(a) and (b) reveal that the final time 55 is already in the nonlinear stage of the evolution. We also find that the growth of the parallel energy coincides with those of the other two components only in short period at $40 < t < 45$, or rather faster than them. As is commented in the above, the final period of this simulation is influenced by nonlinear coupling in the MHD equations. Deviations of the parallel energy growth from the other two components should be attributed to the nonlinear growth. Based on studies of the growth of separate m/n Fourier modes (figures of which are omitted here), the linear growth is considered in between $t \simeq 30$ and $t \simeq 40$.

In Fig.2, the growth rates obtained in this simulation are compared to the ideal linear analysis. The CAS3D3[**?**] computation provides estimates of the growth rates. The growth rates for $n \leq 4$ in the simulation shows reasonable coincidence to the CAS3D computation. Compared to our previous work[5], the number of grid points are doubled into the two directions of a poloidal cross-section. Although the parameters are the same as the ones in the previous work, the artificial dissipations due to the truncation is drastically decreased thanks to the high resolution properties of the compact scheme.[10] Nonetheless, we still have to recognize that the moderate Fourier modes $n > 7$ is under the influence of the dissipative coefficients. We also note that $\mu = 1 \times 10^{-6}$ is the minimum value which makes sense as a *physical* viscosity for the current numerical resolution. Although we could reduce the viscosity below 1×10^{-6}, the growth of unstable modes becomes rather insensitive to the change of μ, suggesting that the numerical viscosity associated with the truncation errors become gradually dominant.

3 Nonlinear evolution

Next, the nonlinear evolutions of the instability is studied by the simulation with the parameter set (B). In Fig.3, the time evolution of the volume-integrated amplitudes of the three vector components of the velocity vector field are shown. The growth rate of the parallel flow component is the same as the other two component, making a difference to the observation in Fig.Fig:Run553total. It shows that the three components obey to the same kind of the instability. Among the three components of the velocity vector, the parallel component becomes dominant finally even though it is initially much smaller than the other two components.

Fourier amplitudes for some toroidal Fourier modes n of (a) the normal, (b) the binormal and (c) the parallel components of the velocity vector are shown in Figs.4(a)-(c), respectively. In Figs.4(a) and (b), Fourier amplitudes associated with the odd toroidal numbers $n = 1$, 3, 5, 7, 9, and 11 grows the fastest. The growth of the Fourier modes are mostly contributed by the Fourier mode set m/n associated with the $\iota/2\pi = 0.5$ rational surface. Growth rates of these Fourier modes are almost identical. Although the separation between odd and even wavenumbers are not clarified yet, the exponential growth of the even toroidal numbers are considered as a consequence of nonlinear couplings of the odd wavenumbers rather than their own linear instability, since the growth rates of these even numbers are as large as the twice of the growth rates of the odd numbers. Among the four dissipative coefficients, the parallel heat conductivity κ is considered as the most influencing one. For example, once the unstable Fourier modes which are resonant to the $\iota/2\pi = 0.5$ rational surface grow, the pressure distribution is modified because of the large $\kappa_{//}$. Since eigen-functions of low n modes cover wide are across the flux surfaces, the $\kappa_{//}$ effect can also modify the pressure profile in wide area. In Fig.4(c) the time evolutions of the Fourier amplitudes of the parallel velocity component are shown. In comparison to Figs.4(a) and (b) in which the toroidal modes $n = 1$, 3 and 5 have almost the same amplitudes, it is clearly seen that the $n = 1$ Fourier mode achieves the largest amplitude. Furthermore, there is no clear distinction between even and odd mode numbers.

In Fig.5, the pressure isosurfaces and contours on a poloidal cross-sections are shown at $t = 110\tau_A$ (upper) and $150\tau_A$ (lower). At $t \simeq 110\tau_A$, many of the Fourier modes are saturated or going to be saturated. The contour lines on the poloidal cross-section in Fig.5(a) exhibits clear

mushroom-like structures. The mushroom-like structures have been repeatedly reported in our earlier works.[4, 5, 6] While the structures in the earliest work consist mainly of $m/n = 2/1$ Fourier modes, the structure in this article consist of many more Fourier modes which are resonant to the $\iota/2\pi = 0.5$ surface. The overlapping of the resonant modes provides quite large pressure deformation. Consequently, the contour plots of the pressure (and therefore the Poincare plots of the magnetic field lines, which are not shown here, too) become quite chaotic after the nonlinear saturations. However, at $t = 150\tau_A$, the pressure contour associate with the outermost closed surface is not deformed very much through the linear and nonlinear evolution, suggesting that the confinement is not critically damaged in spite of the strong instability. Furthermore, contour lines tend to form the concentric profiles again, showing a possibility of organizing relatively well confined state again.

4 Concluding Remarks

Direct numerical simulation study is conducted to study linear and nonlinear evolution of the instability in LHD. A simulation with relatively small dissipative coefficients shows good coincidence of the linear growth rates with the ideal analysis. In nonlinear simulations, the parallel flow becomes dominant after the nonlinear saturation. It is noteworthy that the parallel flow tends to grow much larger than the other two components of the velocity vector in the simulation with smaller dissipative coefficients than in the one with larger coefficients. It suggests that the parallel flow dominance is much stronger in simulations with very small dissipative coefficients. The numerical simulations in this work was carried out on NEC SX-7 "Plasma Simulator" in National Institute for Fusion Science under the NIFS program NIFS06KTA033.

[1] K. Watanabe et al., Nucl. Fusion **45**, 1247 (2005).
[2] H. Miura et al., Phys. Plasmas **8**, 4870 (2001)
[3] K. Ichiguchi et al., Nucl. Fusion **43** 1101 (2003).
[4] H. Miura et al., IAEA-CSP-25/CD/TH/2-3 (2004).
[5] H. Miura et al., AIP Conference Proceedings **871** (2006).
[6] H. Miura et al., Fusion Science and Technology **51**, 8 (2007).
[7] C.Nührenberg, Phys. Plasmas **6** 137 (1999).
[8] N. Nakajima, *Phys. Plasmas* **3** 4556 (1996).
[9] C. Nührenberg, *Phys. Plasmas*, **6** 137 (1999).
[10] S.K. Lele, *J. Compu. Phys.* **103** 16 (1992).

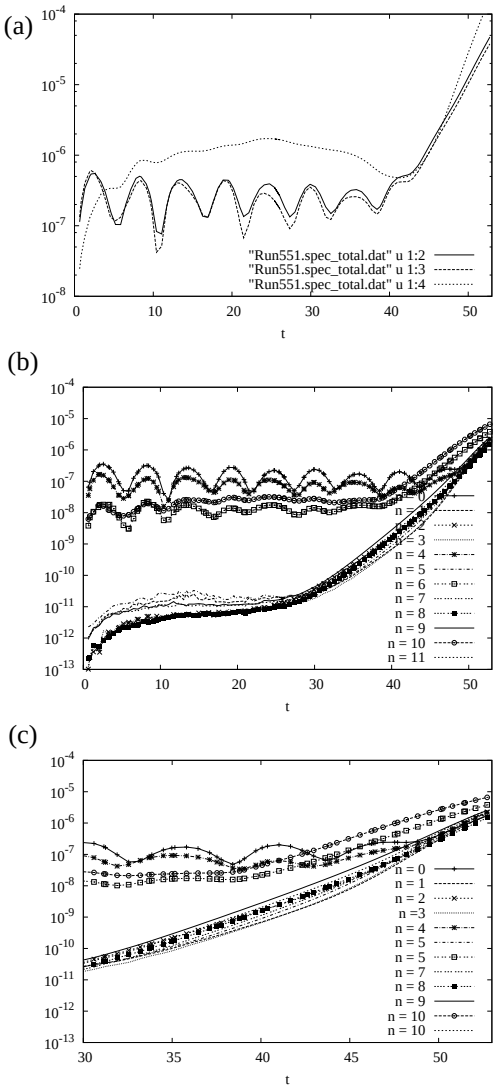

Fig. 1 Time evolutions of (1)the volume-integrated energy of the three components of the velocity vector, (b)the Fourier amplitudes of the normal velocity component $A_{\nabla\phi,n}$, and (c) an magnification of (b), in the parameter set (A) simulation.

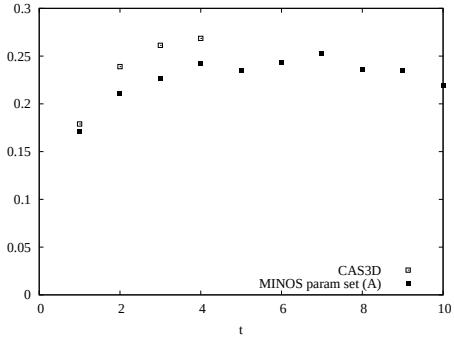

Fig. 2 Comparison of the growth rates of the Fourier amplitudes in the parameter set (A) simulation to those of the CAS3D computations.

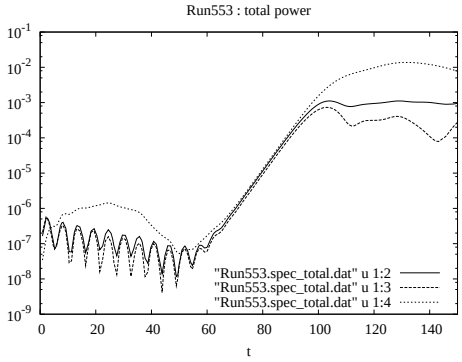

Fig. 3 Time evolutions of the Fourier amplitudes of the normal velocity component in the parameter set (B) simulation.

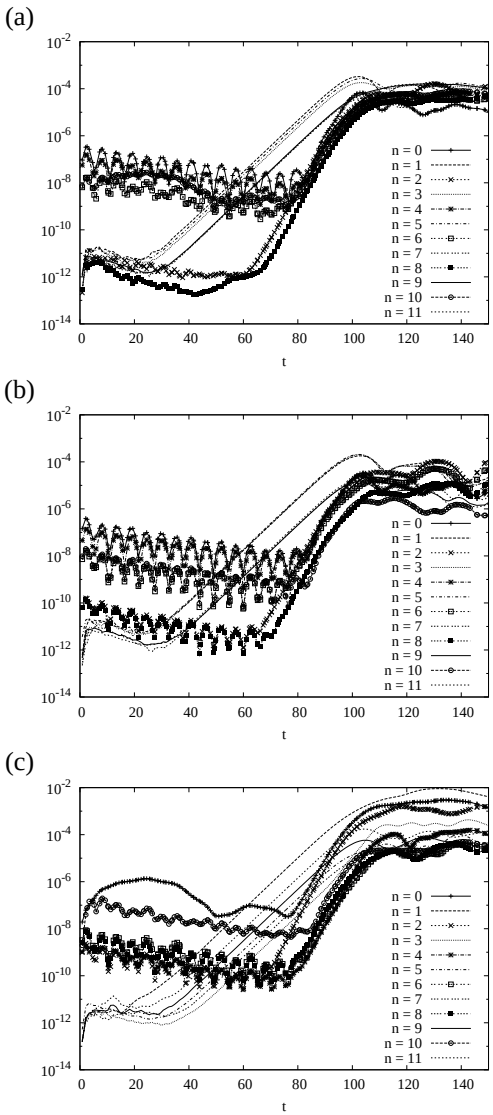

Fig. 4 Time evolutions of the Fourier amplitudes of (a)the normal, (b) the binormal and (c) the parallel velocity components in the parameter set (B) simulation.

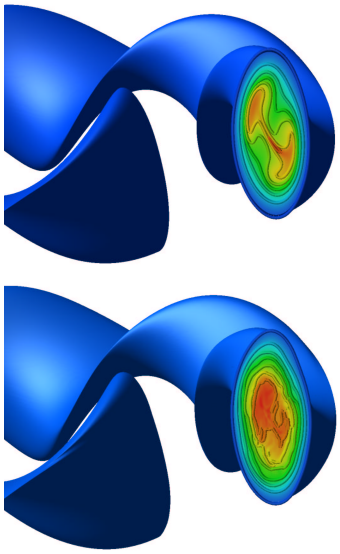

Fig. 5 Isosurfaces and contours of the pressure on a vertically-elongated poloidal cross-sections at $t = 110\tau_A$ (upper) and $150\tau_A$ (lower). At the midst of the two times, the contour lines of the pressure are much more chaotic. After the destruction of the closed contour lines, concentric profiles of the pressure tend to be recovered.